Title:
Enhancing the Quality of Non-Uniform Degenerate Patches in Unstructured T-Splines via Degree Elevation

Authors:
Sheng Lei, leeeeeis_buaa@buaa.edu.cn, Beihang University
Gang Zhao, zhaog@buaa.edu.cn, Beihang University
Wei Wang, jrrt@buaa.edu.cn, Beihang University
Xiaoxiao Du, duxiaoxiao@buaa.edu.cn, Beihang University
Pengfei Han, hanpf@buaa.edu.cn, Beihang University

Keywords:
Degenerate Patch, Degree Elevation, Unstructured T-Splines, Isogeometric Analysis

DOI: 10.14733/cadconfP.2026.26-31

Introduction:
In the field of CAD, the representation of high quality free-form surfaces with arbitrary topological structures is a long-standing problem. After the appearance of T-splines and isogeometric analysis (IGA), combining the two to provide analysis-suitable complex geometry models is possible, while to enhance the quality of the surface models, two continuity improving approaches are eligible: parametric continuity methods [7, 5, 9, 1] and geometric continuity methods [4, 6, 2, 3]. Parametric continuity methods can achieve accurate refinements of surfaces in the neighborhood of singular points, exhibit optimal convergence in IGA, and have been validated on relatively complex models. Consequently, ensuring parameter continuity has become a central issue in the study of unstructured spline surface, particularly for achieving smooth surface joining under arbitrary topologies.

The most commonly used method for improving continuity in the neighborhood of extraordinary points (EP) on unstructured spline surfaces is the D-patch method. While the method can achieve C^1 continuity in the neighborhoods of EPs, it simultaneously leads to a significant degradation in surface quality. In this work, we propose a local degree-elevation-based framework that significantly improves surface quality near EPs, while preserving C^1 continuity and full compatibility with non-uniform ASUT-splines, ultimately constructing local higher-order unstructured splines. The effectiveness of the proposed method is demonstrated by several examples through visual rendering, zebra-stripe analysis and convergence studies, which indicate a clear improvement in surface quality.

Degenerate Patch:
In 2012, Scott et al. [8] formally introduced the concept of unstructured T-splines based on Bézier extraction. After that, the ASUT-splines [1, 10] are explored in depth for applications in IGA, with the method to improve the continuity in the neighborhoods of EPs as one of the research focuses. All studies on parameter continuity in ASUT-spline theory utilize the two D-patch smoothing matrices derived under the uniformity assumption, as provided by Reif [7]. The neighborhood is typically composed of μ bi-cubic Bézier patches $\boldsymbol{s}^i$ $(i = 0, 1, ..., \mu - 1)$ using the Bézier extraction algorithm

$\boldsymbol{s}^i(u,v) = \sum_{r=0}^{3}\sum_{t=0}^{3} \boldsymbol{b}_{rt}^i B_{r,t}(u,v)$, $u \in [0, U^i], v \in [0, V^i]$ where $\boldsymbol{b}_{rt}^i$ are Bézier points of $\boldsymbol{s}^i$, $B_{r,t}$ are bi-cubic Bernstein basis functions and obviously $V_i = U_{i+1}$. To maintain C^1 continuity at an EP of valence μ, constraints can be written as follows,

$$\boldsymbol{s}^i(0,l) = \boldsymbol{s}^{i+1}(l,0), \quad \frac{\partial}{\partial u}\boldsymbol{s}^i(0,l) = -\frac{\partial}{\partial v}\boldsymbol{s}^{i+1}(l,0) \tag{2.1}$$

These constraints form a system of cyclic equations. The degenerate patch (D-patch) framework provides a rigorous mathematical basis for resolving the singularity and continuity issues at EPs. The smoothing matrix $\mathbf{\Pi}$ ($\mathbf{\Pi}^{U,\circ}, \mathbf{\Pi}^{U,+}$ and $\mathbf{\Pi}^{N,\circ}$) is the linear operator that maps a set of initial quasi-control points $\tilde{\boldsymbol{B}}$ to the constrained control points $\boldsymbol{B}$ that satisfy the D-patch requirements. Formally, $\mathbf{\Pi}$ must satisfy affine invariance and span the nullspace of the C^1 continuity constraints. By integrating the non-uniform D-patch framework with the smoothing matrices above, [11] establishes a robust pipeline for ASUT-splines. However, despite its theoretical advantages, the D-patch construction often leads to noticeable surface quality degradation in the neighborhoods of EPs, as illustrated in Fig.1.

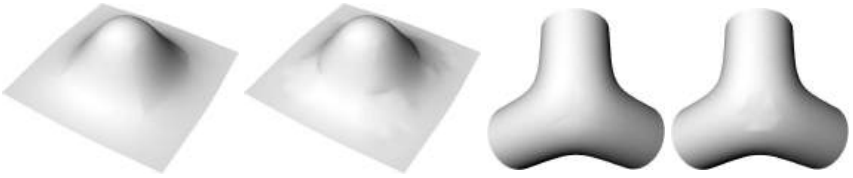

Fig. 1: Comparison of the Bézier extraction C^0 results and D-patches using matrix $\mathbf{\Pi}^{U,\circ}$ in two unstructured T-splines models

Degree Elevation and Continuity Improvement:

To address the surface quality limitations of the existing bi-cubic D-patch constructions, we implement a so-called EEDS (extraction-elevation-degeneration-smooth) pipeline for processing the local neighborhoods of EPs. Considering the unstructured T-spline surface as input, our algorithm consists of four steps:

- Bézier extraction to obtain C^0-continuous patches in the EP neighborhood

For all surface patches except those 2-ring patches of EPs, the blending functions and control points that influence them can be determined by examining the local knot span vectors of the surrounding vertices, thus obtaining the element representation form. For the 2-ring patches of an EP, the Bézier extraction algorithm for a quadrilateral mesh [8] is used to construct the expression for each element. First, a linear relationship between the control points is defined, then an extraction matrix is constructed, and finally, the transformation relationship between the spline basis functions and the Bernstein basis functions is obtained. The two algorithms have opposite approaches, but both yield the same result.

- Split and degree elevation of 1-ring patches of an EP

To reduce the area of the surface affected by degeneration, the 1-ring bi-cubic Bézier patches of EPs obtained by Bézier extraction algorithm need to be precisely 2×2 split along the center of their parameter domains. Subdividing a bi-cubic Bézier surface at the parameter center $(u = 0.5, v = 0.5)$ into four sub-surfaces is essentially a two-dimensional application of the De Casteljau algorithm. For a cubic curve, splitting it at $t = 0.5$ results in two sets of control points. This is represented by two 4×4

splitting matrices $\boldsymbol{S}_1$ for the left half and $\boldsymbol{S}_2$ for the right half. Similar to subdividing the surface into four quadrants, we apply these splitting matrices to both the u and v directions of the 4×4 control point grid. Store the control points as $\boldsymbol{P}$ in the *u-then-v* order, the transformation for each sub-surface can be written as a single 16×16 matrix $\boldsymbol{W}_k$ to satisfy $\boldsymbol{Q}_k = \boldsymbol{W}_k \boldsymbol{P}, \quad k \in \{LL, LR, UL, UR\}$ where $\boldsymbol{W}_{LL} = \boldsymbol{S}_1 \otimes \boldsymbol{S}_1, \boldsymbol{W}_{LR} = \boldsymbol{S}_1 \otimes \boldsymbol{S}_2, \boldsymbol{W}_{UL} = \boldsymbol{S}_2 \otimes \boldsymbol{S}_1, \boldsymbol{W}_{UR} = \boldsymbol{S}_2 \otimes \boldsymbol{S}_2$.

Degree elevation increases the polynomial degree of the underlying Bernstein basis while preserving the exact geometry of the Bézier surface. Mathematically, it is achieved by expressing the original surface in terms of a higher-order Bernstein basis. To elevate a Bézier curve from degree $p = 3$ to a target degree k ($k > 3$), we define a transformation matrix $\boldsymbol{M}$ of size $(k+1) \times 4$ that $\boldsymbol{M}_{i,j} = \binom{3}{j}\binom{k-3}{i-j}/\binom{k}{i}$.

A Bézier surface is a tensor product construction, which means the elevation can be performed independently along the u-parameter and v-parameter directions. If we represent the initial 4×4 control points as a bi-cubic grid, the elevation to degree $m \times n$ follows this logic: (i) apply the u-direction elevation matrix $\boldsymbol{M}_u$ of size $(m+1) \times 4$ to each column of the grid and (ii) apply the v-direction elevation matrix $\boldsymbol{M}_v$ of size $(n+1) \times 4$ to each row of the resulting intermediate grid. When the control points are organized into a single column matrix $\boldsymbol{P}$ (16×3), we use the Kronecker Product ($\otimes$) to represent the simultaneous transformation in both directions. If the points in $\boldsymbol{P}$ are ordered in the *u-then-v* order, the relationship is $\boldsymbol{Q} = (\boldsymbol{M}_v \otimes \boldsymbol{M}_u)\boldsymbol{P}$. In this paper, each Bézier patch of 1-ring face in a UT-splines is required to be elevated into bi-quintic.

- Patch degeneration

After split and degree elevation, each 1-ring face of the UT-splines contains four bi-quintic Bézier patches, which have more internal control points. Compared to bi-cubic patches, bi-quintic D-patches allow for more flexibility in optimizing the surface shape while satisfying C^1 continuity constraints, avoiding sharp or wrinkled features near the EPs. Theoretically, smoothing matrices $\boldsymbol{\Pi}^{U,\circ}$ and $\boldsymbol{\Pi}^{U,+}$ can be used to handle situations where the intervals on the spoke edges of EPs are non-uniform, but this leads to certain limitations. Therefore, we use the non-uniform smoothing matrix $\boldsymbol{\Pi}^{N,\circ}$ [11] to perform the degeneration process on the bi-quintic Bézier patches.

Using the feasible constant set $\lambda = \left\{\alpha^i, \beta^i, \gamma^i, \delta^i : i = 0, 1, ..., \mu - 1\right\}$ that $\alpha^i = 1 - \frac{V^i}{U^i}\beta\cos\varphi_\mu$, $\beta^i = \frac{V^i}{U^i}\beta$, $\gamma^i = \frac{U^i}{V^i}\beta$, $\delta^i = 1 - \frac{U^i}{V^i}\beta\cos\varphi_\mu$ where $\beta \in \mathbb{R}^+, \varphi_\mu = 2\pi/\mu$, and the idempotent non-uniform smoothing matrix $\boldsymbol{\Pi}^{N,\circ}$ is designed as

$$\boldsymbol{\Pi}^{N,\circ} = \frac{1}{D}\begin{bmatrix} \boldsymbol{\Pi}_1^{N,\circ} & \boldsymbol{\Pi}_2^{N,\circ} & \boldsymbol{\Pi}_3^{N,\circ} \\ \left(\boldsymbol{\Pi}_2^{N,\circ}\right)^T & \boldsymbol{\Pi}_5^{N,\circ} & \boldsymbol{\Pi}_6^{N,\circ} \\ \left(\boldsymbol{\Pi}_3^{N,\circ}\right)^T & \left(\boldsymbol{\Pi}_6^{N,\circ}\right)^T & \boldsymbol{\Pi}_9^{N,\circ} \end{bmatrix} \tag{2.2}$$

We can project the arbitrary control points $\left\{\boldsymbol{q}_{11}^i, \boldsymbol{q}_{21}^i, \boldsymbol{q}_{12}^i : i = 0, 1, ..., \mu - 1\right\}$ of bi-quintic Bézier patches to obtain quasi control points that satisfy the D-patch conditions, ensuring C^1 continuity across the spoke edges.

- Adaptive adjustment and Laplacian smoothing

After processing the control points involved in cyclic constraints, the remaining control points involved in continuity constraints can be easily decoupled in the constraint equations. We achieve complete C^1 continuity across the spoke edges by adjusting the boundary control points of each Bézier patch.

As mentioned above, for each of the bi-quintic patches, excluding the constrained control points, the central region will have four internal control points (typically indexed as $\boldsymbol{q}_{22}^i, \boldsymbol{q}_{32}^i, \boldsymbol{q}_{23}^i, \boldsymbol{q}_{33}^i$). These points

provide a certain degrees of freedom to optimize the smoothness of the patch interior without disrupting boundary continuity. To implement Laplacian smoothing for the 4 inner control points of a bi-quintic Bézier patch, we leverage the fact that these points are not constrained by the C^1 boundary conditions.

The goal of Laplacian smoothing is to ensure that each interior point lies at the centroid of its immediate topological neighbors. For a structured grid, the discrete Laplace's equation is

$$\Delta \boldsymbol{q}_{i,j} = 4\boldsymbol{q}_{i,j} - (\boldsymbol{q}_{i-1,j} + \boldsymbol{q}_{i+1,j} + \boldsymbol{q}_{i,j-1} + \boldsymbol{q}_{i,j+1}) = 0 \tag{2.3}$$

By applying the operator to the four target points, we derive a coupled system because these points are neighbors of one another. We separate the unknown interior points from the known boundary and ribbon points and rewrite the system of equations as a compact linear system. It minimizes the tension within the patch, preventing visual artifacts like bulges or flat spots near the EPs. It respects the C^1 constraints while utilizing the higher-order degrees of freedom to optimize the internal shape.

Figure 2 fully illustrates the processing flow of the method presented in this paper.

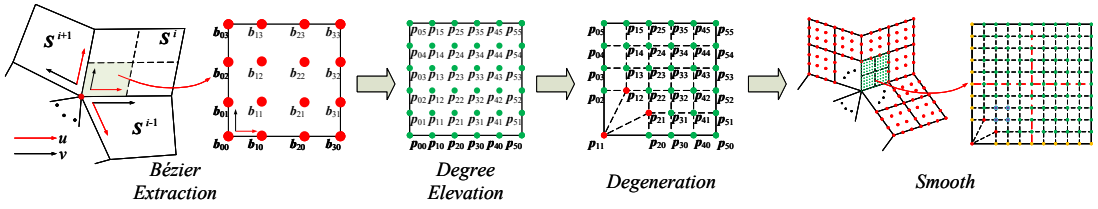

Fig. 2: The processing flow of the proposed EEDS method

Numerical Examples:

Several numerical examples are presented in Fig.3 to evaluate the proposed EEDS pipeline, with direct comparisons to the existing bi-cubic D-patch constructions under both uniform and non-uniform knot configurations. The examples focus on unstructured T-spline models containing uniform (the first, third and fourth examples) or non-uniform (the second example) spoke edges and EPs of different valences, which are well known to be challenging cases for classical C^1 continuity constructions. Surface quality is assessed using visual rendering and zebra stripe analysis, which are particularly sensitive to curvature irregularities near EPs.

The convergence of isogeometric analysis of an unstructured T-spline surface using the EEDS pipeline is studied. The initial surfaces are designed to obtain 2, 3 and 5 EPs respectively. To implement Kirchhoff-Love shell analysis, it is required that the shape functions across the elements satisfy at least C^1 continuity. Consequently, the initial surfaces smoothed by the EEDS scheme and the resulted surfaces obtained under the globally uniform refinement are tested by the following problem of Poisson's equation

$$\text{find } u : \Omega \to \mathbb{R} : \begin{cases} -\Delta u = g & \text{in } \Omega, \\ u = 0 & \text{on } \partial\Omega. \end{cases} \tag{2.4}$$

on the unit square $\Omega = (0,1)^2$ with $g = 2\pi^2 \sin(\pi x)\sin(\pi y)$ and the exact solution $u = \sin(\pi x)\sin(\pi y)$. The numerical accuracy is quantified by computing the errors between the exact solution u and the numerical approximations. The convergence results for the three unstructured meshes under globally uniform refinement are plotted in Fig.4. For each mesh configuration, the numerical solution is computed on a sequence of uniformly refined grids, and the errors $\|u^i - u\|$ are reported in the L^2, L^∞ and H^1 norms against the total number of degrees of freedom (DOF). It demonstrates that the numerical errors systematically decrease at rapid rates under refinement strategies.

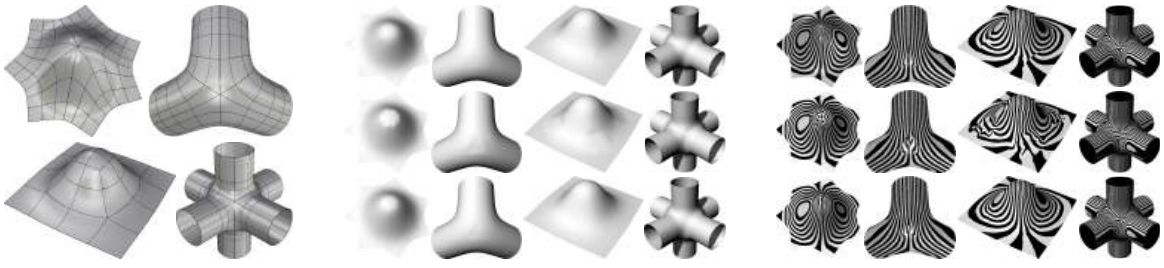

(a) Unstructured meshes (b) Rendering results of the models (c) Zebra-stripes of the models

Fig. 3: Unstructured meshes with uniform or non-uniform spoke edges and results of different models, in each column from top to bottom: the results of C^0, bi-cubic D-patch, and EEDS

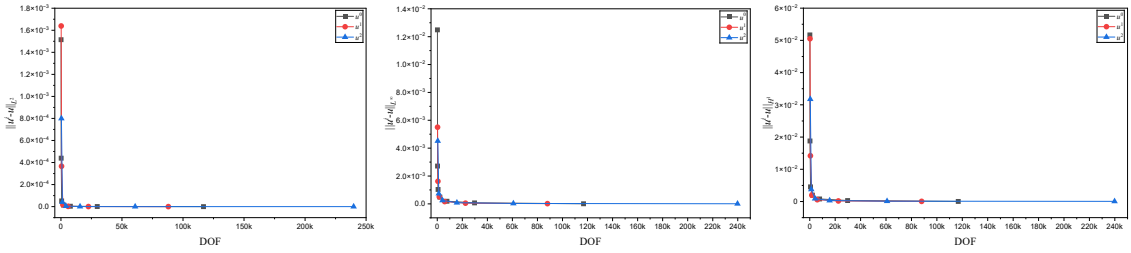

Fig. 4: Convergence study of EEDS, errors in the L^2, L^∞ and H^1 norms from left to right

It is worth noting that the improvement in surface quality is achieved without altering the global structure of the unstructured T-spline by introducing additional EPs. All operations are strictly local to the 1-ring neighborhood of each EP, and the use of the idempotent non-uniform smoothing matrix $\mathbf{\Pi}^{N,\circ}$ ensures compatibility with non-uniform spoke edges. The final Laplacian smoothing step further enhances the interior shape of each bi-quintic patch while preserving all C^1 continuity constraints. Since all operations are strictly local and preserve the underlying spline space structure, the proposed method does not affect the analysis-suitability of ASUT-splines.

Conclusions:

This paper presents a localized EEDS framework for improving surface quality in the neighborhoods of EPs in unstructured T-splines. By locally elevating 1-ring Bézier patches to bi-quintic level and utilizing unconstrained interior degrees of freedom, the method effectively alleviates surface artifacts such as dimples and flat regions compared to the existing bi-cubic D-patch constructions. Visual rendering, zebra stripe analysis and isogeometric convergence studies demonstrate that the proposed approach significantly improves geometric fairness. Furthermore, the incorporation of a non-uniform idempotent smoothing matrix ensures the framework maintains robust convergence behavior and full compatibility with analysis-suitable unstructured T-splines without altering the global topology. Future work will focus on extending the framework toward higher-order continuity (e.g., C^2 constructions), exploring advanced optimization strategies for interior control points, and theoretically investigating the approximation properties and error distribution of locally elevated patches.

Acknowledgement:

This work is supported by National Key Research and Development Program of China (Project No.

2023YFB3309000), National Natural Science Foundation of China (Project Nos. 52175213, 62102012 and 61972011), Beijing Natural Science Foundation (Project No. 4242025) and Young Elite Scientists Sponsorship Program by CAST (Project No. 2022QNRC001).

Sheng Lei, https://orcid.org/0009-0001-4873-4447
Gang Zhao, https://orcid.org/aaaa-bbbb-cccc-dddd
Wei Wang, https://orcid.org/0000-0002-5089-0000
Xiaoxiao Du, https://orcid.org/0000-0002-2324-1005
Pengfei Han, https://orcid.org/0000-0003-0558-4773

References:

[1] Casquero, H.; Wei, X.; Toshniwal, D.; Li, A.; Hughes, T.-J.; Kiendl, J.; Zhang, Y.-J.: Seamless integration of design and Kirchhoff-Love shell analysis using analysis-suitable unstructured T-splines, Computer Methods in Applied Mechanics and Engineering, 360, 2020, 112765. https://doi.org/10.1016/j.cma.2019.112765

[2] Kapl, M.; Buchegger, F.; Bercovier, M.; Juttler, B.: Isogeometric analysis with geometrically continuous functions on planar multi-patch geometries, Computer Methods in Applied Mechanics and Engineering, 316, 2017, 209-234. https://doi.org/10.1016/j.cma.2016.06.002

[3] Kapl, M.; Sangalli, G.; Takacs, T.: Isogeometric analysis with C^1 functions on planar, unstructured quadrilateral meshes, The SMAI journal of computational mathematics, 5, 2019, 67-86. https://doi.org/10.5802/smai-jcm.52

[4] Nguyen, T.; Karciauskas, K.; Peters, J.: A comparative study of several classical, discrete differential and isogeometric methods for solving Poisson's equation on the disk, Axioms, 3(2), 2014, 280-300. https://doi.org/10.3390/axioms3020280

[5] Nguyen, T.; Peters, J.: Refinable C1 spline elements for irregular quad layout, Computer aided geometric design, 43, 2016, 123-130. https://doi.org/10.1016/j.cagd.2016.02.009

[6] Peters, J.; Peters, J.: Matched G^k-constructions yield C^k-continuous iso-geometric elements, arXiv preprint arXiv:1406.4229, 2014. https://doi.org/10.48550/arXiv.1406.4229

[7] Reif, U.: A refineable space of smooth spline surfaces of arbitrary topological genus, Journal of Approximation Theory, 90(2), 1997, 174-199. https://doi.org/10.1006/jath.1996.3079

[8] Scott, M.-A.; Simpson, R.-N.; Evans, J.-A.; Lipton, S.; Bordas, S.-P.; Hughes, T.-J.; Sederberg, T.-W.: Isogeometric boundary element analysis using unstructured T-splines, Computer Methods in Applied Mechanics and Engineering, 254, 2013, 197-221. https://doi.org/10.1016/j.cma.2012.11.001

[9] Toshniwal, D.; Speleers, H.; Hughes, T.-J.: Smooth cubic spline spaces on unstructured quadrilateral meshes with particular emphasis on extraordinary points: Geometric design and isogeometric analysis considerations, Computer Methods in Applied Mechanics and Engineering, 327, 2017, 411-458. https://doi.org/10.1016/j.cma.2017.06.008

[10] Wei, X.; Li, X.; Qian, K.; Hughes, T.-J.; Zhang, Y.-J., Casquero, H.: Analysis-suitable unstructured T-splines: Multiple extraordinary points per face, Computer Methods in Applied Mechanics and Engineering, 391, 2022, 114494. https://doi.org/10.1016/j.cma.2021.114494

[11] Yang, J.; Zhao, G.; Wang, W.; Du, X.; Zuo, C.: Non-uniform C1 patches around extraordinary points with applications to analysis-suitable unstructured T-splines, Computer Methods in Applied Mechanics and Engineering, 405, 2023, 115849. https://doi.org/10.1016/j.cma.2022.115849